Journal Pre-proof

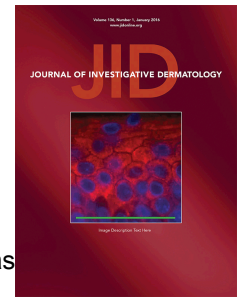

GPR119 is a potent regulator of human sebocyte biology

Arnold Markovics, Ágnes Angyal, Kinga Fanni Tóth, Dorottya Ádám, Zsófia Pénzes, József Magi, Ágnes Pór, Ilona Kovács, Dániel Törőcsik, Christos C. Zouboulis, Tamás Bíró, Attila Oláh

PII: S0022-202X(20)30222-0

DOI: https://doi.org/10.1016/j.jid.2020.02.011

Reference: JID 2328

To appear in: *The Journal of Investigative Dermatology*

Received Date: 12 July 2018

Revised Date: 31 January 2020

Accepted Date: 12 February 2020

Please cite this article as: Markovics A, Angyal Á, Tóth KF, Ádám D, Pénzes Z, Magi J, Pór Á, Kovács I, Törőcsik D, Zouboulis CC, Bíró T, Oláh A, GPR119 is a potent regulator of human sebocyte biology, *The Journal of Investigative Dermatology* (2020), doi: https://doi.org/10.1016/j.jid.2020.02.011.

GPR119 is a potent regulator of human sebocyte biology

Arnold Markovics[1,2*], Ágnes Angyal[1,2*], Kinga Fanni Tóth[1,2], Dorottya Ádám[1,2], Zsófia Pénzes[1,2,3], József Magi[1], Ágnes Pór[4], Ilona Kovács[4], Dániel Törőcsik[5], Christos C. Zouboulis[6], Tamás Bíró[7#], Attila Oláh[1#]

[1]Department of Physiology, Faculty of Medicine, University of Debrecen, Debrecen, Hungary; [2]University of Debrecen, Doctoral School of Molecular Medicine, Debrecen, Hungary; [3]Department of Immunology, Faculty of Medicine, University of Debrecen, Debrecen, Hungary; [4]Department of Pathology, Gyula Kenézy University Hospital, University of Debrecen, Debrecen, Hungary; [5]Department of Dermatology, Faculty of Medicine, University of Debrecen, Debrecen, Hungary; [6]Departments of Dermatology, Venereology, Allergology and Immunology, Dessau Medical Center, Brandenburg Medical School Theodor Fontane, Dessau, Germany; [7]DE-MTA "Lendület" Cellular Physiology Research Group, Department of Immunology, Faculty of Medicine, University of Debrecen, Debrecen, Hungary

**These authors contributed equally.*

[#]These authors contributed equally.

Corresponding author:

Attila Oláh, MD, PhD, Department of Physiology, Faculty of Medicine, University of Debrecen; Egyetem square 1. Debrecen, H-4032, Hungary; e-mail: olah.attila@med.unideb.hu; phone: +3652-255-575; FAX: +3652-255-116.

Short title: GPR119 regulates sebocyte biology

Abbreviations: endocannabinoid system, ECS; OEA, oleoylethanolamide; sebaceous gland, SG; T2DM, type 2 diabetes mellitus.

ABSTRACT

We have previously shown that endocannabinoids promote sebaceous lipogenesis, and sebocytes are involved in the metabolism of the "endocannabinoid-like" substance oleoylethanolamide (OEA). OEA is an endogenous activator of GPR119, a recently de-orphanized receptor, which is currently being investigated as a promising anti-diabetic drug target. Thus, in the current study, we investigated the effects of OEA as well as the expression and role of GPR119 in human sebocytes.

We found that OEA promoted differentiation of human SZ95 sebocytes (elevated lipogenesis, enhanced granulation, and the induction of early apoptotic events), and it switched the cells to a pro-inflammatory phenotype (increased expression and release of several pro-inflammatory cytokines). Moreover, we could also demonstrate that GPR119 was expressed in human sebocytes, and its siRNA-mediated gene silencing suppressed OEA-induced sebaceous lipogenesis, which was mediated via JNK, ERK1/2, Akt/PKB, and CREB activation. Finally, our pilot data demonstrated that GPR119 was down-regulated in sebaceous glands of acne patients, arguing that GPR119 signaling may indeed be disturbed in acne.

Collectively, our findings introduce the OEA→GPR119 signaling as a positive regulator of sebocyte differentiation, and highlight the possibility that dysregulation of this pathway may contribute to the development of seborrhea and acne.

INTRODUCTION

The endocannabinoid system (ECS) is a multifaceted signaling network comprising endogenous ligands ("endocannabinoids" [eCBs]), receptors (e.g. CB_1, CB_2, etc.), and a complex enzyme and transport apparatus involved in synthesizing and degrading the eCBs. It regulates several aspects of the homeostasis, including e.g. appetite, lipid accumulation in adipocytes or immune responses (Maccarrone et al. 2015; Oláh et al. 2017b; Solymosi and Köfalvi 2017; Tóth et al. 2019). Moreover, the complex cannabinoid signaling is deeply involved in the regulation of cutaneous physiology as well (Bíró et al. 2009; Maccarrone et al. 2015; Oláh and Bíró 2017; Tóth et al. 2019).

GPR119, a recently de-orphanized "ECS-related" metabotropic receptor, has lately emerged as a promising therapeutic target in type 2 diabetes mellitus (T2DM) (Tyurenkov et al. 2017). Thus, from the point of view of the potential side effects it would be highly desirable to explore extrapancreatic expression of GPR119 in human tissues. According to an early study, GPR119 is expressed at the mRNA level in cultured primary human melanocytes (Scott et al. 2006), and was found to be overexpressed in melanomas as compared to nevi (Haskó et al. 2014; Qin et al. 2011). Intriguingly, however, apart from this, only scant evidence is available on this matter (Alexander 2016).

We have previously shown that several members of the ECS are expressed in human sebaceous glands (SG), and that ECS regulates biology of the human sebocytes (Dobrosi et al. 2008; Oláh and Bíró 2017; Zákány et al. 2018). Indeed, we found that the locally produced prototypic eCBs (i.e. anandamide [AEA] and 2-

arachidonoylglycerol [2-AG]) contributed to the maintenance of the homeostatic sebaceous lipogenesis via activating CB_2 cannabinoid receptor and the ERK1/2 MAPK cascade (Dobrosi et al. 2008). We could also demonstrate that human sebocytes express all the key enzymes involved in the synthesis (e.g. N-acyl-ethanolamine specific phospholipase D [NAPE-PLD], etc.) and degradation (e.g. fatty acid amide hydrolase [FAAH]) of the major eCBs. Moreover, elevation of the eCB tone by pharmacological inhibition of the eCB membrane transporter promoted sebaceous lipogenesis, and resulted in anti-inflammatory effects (Zákány et al. 2018). Intriguingly, however, in contrast to the "classical" eCB signaling, activation of multiple ionotropic cannabinoid receptors belonging to the transient receptor potential (TRP) channel superfamily (namely TRPV1, TRPV3, and TRPV4) suppressed sebaceous lipogenesis (Oláh et al. 2014; Szántó et al. 2019; Tóth et al. 2009), and induced a pro-inflammatory response (TRPV3) (Szántó et al. 2019), whereas plant-derived cannabinoids were proven to exert differential effects on human sebocytes (Oláh et al. 2016b; Oláh et al. 2014). Besides, we have also demonstrated that sebocytes are involved in the metabolism of the "eCB-like" substance oleoylethanolamide (OEA) (Zákány et al. 2018) the most important endogenous activator of GPR119 (Alexander 2016). These data raised the possibility that the major cellular target of OEA, i.e. the aforementioned GPR119, may also be expressed in human SGs (Zákány et al. 2018). Thus, in the current study, we aimed to challenge this hypothesis, and, in the regrettable lack of appropriate animal model systems, investigated human SZ95 sebocytes, a widely accepted model system to study human SG biology (Szöllősi et al. 2017; Tóth et al. 2011; Zouboulis et al. 2014; Zouboulis et al. 2008; Zouboulis et al. 1999).

RESULTS

OEA Promotes Differentiation Of Human Sebocytes

"Classical" eCBs (i.e. AEA and 2-AG) as well as arachidonic acid (AA) typically promote sebaceous lipogenesis of SZ95 sebocytes at 30-50 μM in course of 24-48-hr treatments (Dobrosi et al. 2008; Géczy et al. 2012; Markovics et al. 2019; Oláh et al. 2016b; Oláh et al. 2014; Szántó et al. 2019; Tóth et al. 2009; Zákány et al. 2018). Thus, first, we tested the effects of OEA at the 10 nM – 50 μM concentration range. We showed that, although up to 50 μM the endogenous GPR119 activator OEA did not influence viability (MTT-assay; **Supplementary Figure S1a-b**), or proliferation of SZ95 sebocytes (CyQUANT-assay; **Supplementary Figure S2**), it concentration-dependently (1-50 μM) and significantly increased sebaceous lipogenesis (24- and 48-hr treatments; Nile Red; **Figure 1a-b**), and it also enhanced granulation of sebocytes (48-hr treatments; flow cytometry – side scatter; **Figure 1c**). These data suggested that, similar to the "classical" eCBs (Dobrosi et al. 2008; Zákány et al. 2018), OEA is also able to promote differentiation of human sebocytes. Notably, lipogenic potential of OEA was comparable to the ones typically seen in case of "classical" eCBs (e.g. AEA [30 μM]), AA (50 μM), or the combination of linoleic acid and testosterone (LA+T; 100 μM + 1 μM, respectively) (Dobrosi et al. 2008; Géczy et al. 2012; Makrantonaki and Zouboulis 2007; Markovics et al. 2019; Oláh et al. 2016b; Oláh et al. 2014; Szántó et al. 2019; Tóth et al. 2009; Zákány et al. 2018) (48-hr treatments; **Figure 1d**).

Since, besides the enhanced granulation and elevated sebaceous lipogenesis, programmed cell death is also a hallmark of this process (Zouboulis et al. 2014), next, we asked if OEA influences the ratio of apoptotic or necrotic cells. We found that 48-hr

OEA treatment led to a small, but significant decrease of the mitochondrial membrane potential, indicating the onset of early apoptotic processes, whereas the ratio of necrotic cells remained unchanged (**Figure 1e**). This suggests that OEA is indeed likely to induce differentiation of human sebocytes.

OEA Induces Pro-Inflammatory Response In Human Sebocytes

To further dissect how OEA influences sebocyte biology, we tested its effects on the immune behavior of these cells. We found that administration of OEA (50 μM; 3 hrs) induced a significant up-regulation of several key pro-inflammatory cytokines (*interleukin [IL]-1α*, *IL-1β*, *IL-6*, *IL-8*; Q-PCR), and increased the release of IL-6 and IL-8 (ELISA) (**Figure 2a-f**). Although the above effects were inferior to the ones of the pro-inflammatory positive control Toll-like receptor 4 activator lipopolysaccharide (**Figure 2a-f**), our data indicate that, besides promoting differentiation, administration of OEA results in a rather pro-inflammatory sebocyte phenotype.

Lipogenic Effect Of OEA Is Not Mediated Via PPARα

Next, we assessed the mechanism of the above differentiation-promoting effects. PPARs are central orchestrators of lipid synthesis, and are expressed in human sebocytes as well (Zouboulis et al. 2014). Since OEA is known to be able to activate PPARα (Fu et al. 2003), next, we investigated if this nuclear receptor is involved in mediating its lipogenic action. Of great importance, we found that, although it tended to suppress it, the selective PPARα antagonist GW 7461 (1 μM) had no significant effect on the OEA-induced lipogenesis (48-hr treatments; **Figure 3a**), making PPARα an unlikely candidate to orchestrate OEA-induced sebaceous lipogenesis.

Human Sebocytes Express GPR119 Both *In Vitro* And *In Situ*

Considering that not only PPARα, but also GPR119 was described to mediate cellular effects of OEA, next we investigated if this receptor is expressed in human sebaceous glands. We showed that GPR119 was expressed in human sebocytes both at the mRNA (Q-PCR) and protein levels (Western blot) (**Figure 3b-c**). Moreover, we also confirmed the presence of the receptor in human SGs *in situ* (immunohistochemistry; **Figure 3d**; appropriate positive control staining of pancreas is presented on **Supplementary Figure S3**). Having evidenced the presence of GPR119, next we assessed its role in regulating SG biology.

Lipogenic Effect Of OEA Is Suppressed By GPR119 Silencing

In the lack of selective antagonists (Alexander 2016), we turned to a molecular biology approach, i.e. siRNA-mediated selective gene silencing. Of great importance, we found that silencing (validated by Q-PCR and Western blot; **Figure 3e-f**) of GPR119 expression significantly suppressed lipogenic action of OEA (**Figure 3g**), confirming that it was indeed a mostly GPR119-mediated effect; however, involvement of the activation of putative GPR119-independent lipogenic pathways cannot be excluded.

Since receptor-mediated actions usually exhibit saturation kinetics, at this point we also tested the effects of higher OEA concentrations (100, 300, and 500 μM) on the lipid synthesis. We found that sebaceous lipogenesis could be further enhanced by 100 and 300 μM of OEA, where it seemed to be saturated (no statistically significant difference could be observed between the lipogenic effect of 100 and 300 μM). However, OEA

was clearly cytotoxic at 500 μM thereby resulting in an artificially low lipid level (24-hr treatments; **Supplementary Figure S4a-b**).

Lipogenic Effect Of OEA Is Mediated Via The Activation Of Several Kinase Cascades

Next, we assessed the effects of OEA on two important, ECS-relevant regulators of sebaceous lipogenesis, i.e. calcium homeostasis and ERK1/2 MAPK cascade (Dobrosi et al. 2008; Oláh et al. 2014). We found that acute OEA administration did not alter $[Ca^{2+}]_{IC}$ (Fluo-4 AM-based fluorescent Ca^{2+}-measurement; **Supplementary Figure S5**), but, similar to the "classical" eCBs (Dobrosi et al. 2008), it activated the ERK1/2 MAPK pathway as revealed by the elevated level of phosphorylated (i.e. activated) ERK1/2 in the OEA-treated cells compared to the vehicle-treated control group (20 min treatments; Western blot; **Figure 4a**). Moreover, the ERK1/2 MAPK inhibitor PD 98059 (10 μM), was able to significantly suppress the lipogenic effect of OEA (24-hr treatments; **Figure 4b**), confirming that activation of this pathway was indeed involved in mediating it. However, it should also be noted that, when applied alone, PD 98059 suppressed basal sebaceous lipid synthesis as well (**Figure 4b**), indicating that this signaling pathway may also be involved in maintaining the homeostatic lipogenesis of human sebocytes.

Considering that GPR119 usually, but not exclusively, exerts its biological effects as a G_s-coupled receptor (Hassing et al. 2016), we also assessed the effects of OEA on the intracellular cAMP level. We found that, although OEA (50 μM; 60 min) tended to increase cAMP level of human sebocytes, this elevation failed to reach statistical

significance (**Figure 4c**). Thus, in order to further dissect its mechanism of action, we turned to a medium-throughput screening method, and used the Proteome Profiler Human Phospho-Kinase Array Kit enabling the simultaneous investigation of several different kinase cascades and related proteins. 20 min treatment of sebocytes with OEA (50 μM) or vehicle revealed that multiple signaling pathways got activated upon OEA treatment, including known lipogenic pathways such as c-Jun N-terminal kinase (JNK)-1/2/3 (Choi et al. 2012; Kwon et al. 2019) or Akt/protein kinase B (PKB) (Choi et al. 2012; Smith et al. 2008), and other molecules (e.g. cAMP response element-binding protein [CREB], Signal Transducers and Activators of Transcription 5 [STAT5], etc.) (summarized in **Table 1**). Importantly, although it tended to suppress it, pharmacological blockade of STAT5 failed to significantly alter OEA-induced lipogenesis (48-hr treatments; **Figure 4d**), whereas inhibition of JNK, CREB, and Akt/PKB could abrogate lipogenic effect of OEA (48-hr treatments; **Figure 4e**).

Taken together, the above data strongly argued that dysregulation of the homeostatic OEA→GPR119 signaling might contribute to the development of sebum overproducing sebaceous gland dysfunctions, e.g. seborrhea or acne, therefore, we decided to assess its expression within the confines of a pilot experiment in SGs of 6 acne patients as well as of 6 acne-free individuals (relevant anamnestic data of the donors are summarized in **Supplementary Table S1**). Of great importance, despite of the relatively low number of participants and the apparently high inter-donor variability, we found that GPR119 expression exhibited a significant decrease in the SGs of acne patients (**Figure 5a-c**) arguing that homeostatic GPR119 signaling might indeed be disturbed in acne at least in a subset of the patients.

DISCUSSION

In the current study, we present evidence demonstrating that i) OEA promotes differentiation of human sebocytes as revealed by elevated sebaceous lipogenesis and cellular granulation (**Figure 1a-c**); ii) it induces early apoptotic processes (**Figure 1e**); and iii) switches the sebocytes to a pro-inflammatory phenotype (**Figure 2a-f**). Importantly, although in case of the inhibition of the eCB membrane transporter, we found that moderate stimulation of sebaceous lipogenesis was accompanied by anti-inflammatory actions (Zákány et al. 2018), coupling of lipogenesis and pro-inflammatory response is not unprecedented. Indeed, we have previously shown that leptin promotes sebaceous lipogenesis and triggers a pro-inflammatory response in human sebocytes via activating STAT3 and the p65 NF-κB pathway (Törőcsik et al. 2014).

When further assessing the mechanism of action, we could also demonstrate that OEA influenced the activity of several second messenger pathways (**Table 1**). Its lipogenic action was independent of PPARα (**Figure 3a**), but could be partially suppressed by silencing of GPR119 (**Figure 3b-g**), as well as by inhibition of ERK1/2, JNK, Akt/PKB, and CREB, whereas pharmacological blockade of STAT5 (which is involved in regulating immune responses in the pilosebaceous unit (Legrand et al. 2016)) had no significant effect (**Figure 4a-e**).

Importantly, although GPR119 usually mediates its actions in a G_s-protein-coupled manner via the elevation of the cAMP level, it is not unprecedented that it may activate alternative signaling pathways, and may exhibit significant signaling bias (Hassing et al.

2016). An obvious candidate mechanism for such actions could be the activation of the β-arrestin pathway, which is not only capable of desensitizing/down-regulating G-protein-coupled receptors, but can also activate the ERK1/2 MAPK cascade (Pouysségur 2000). In line with this, in a recent study, effects of oleoyl-lysophosphatidylinositol on glucagon-like peptide-1 secretion from L-cells were found to be mediated via GPR119, and the subsequent activation of ERK1/2 MAPK as well as the cAMP/PKA/CREB pathways (Arifin et al. 2018), whereas in another study, activation of GPR119 was followed by cAMP accumulation, Ca^{2+}-signal, and ERK1/2 MAPK activation (Zhang et al. 2014). Intriguingly, in our hands, OEA (50 μM) had no effect on the Ca^{2+}-homeostasis of the sebocytes (acute treatment; **Supplementary Figure S5**), and only tended to elevate cAMP level of the sebocytes (60 min; **Figure 4c**). On one hand, the latter might be explained by signaling bias and the activation of alternative second messenger systems. However, considering the well-known compartmentalization of cAMP signaling (Calebiro and Maiellaro 2014), this finding does not necessarily exclude the possibility that cAMP contributes to at least some effects of OEA, since we only tested cAMP levels in whole cell lysates, and did not investigate if cAMP level reaches statistically significant elevation in any subcellular microcompartments upon OEA-treatment.

In line with this argument, activation of CREB (**Table 1**), pharmacological blockade of which was also successful in abrogating lipogenic effect of OEA (**Figure 4e**), is an indirect pointer indicating that cAMP may indeed play a role in mediating certain effects of OEA. However, it is important to emphasize that CREB activation can be achieved not only through the elevation of the cAMP level, but also via alternative

signaling pathways, including, but not limited to Akt/PKB (Du and Montminy 1998). Importantly, Akt/PKB (Choi et al. 2012; Smith et al. 2008), as well as JNK MAPK (Choi et al. 2012; Kwon et al. 2019) are known to mediate lipogenic actions of various mediators in human sebocytes. Moreover, the aforementioned OEA treatment (50 μM, 20 min) was found to activate them (**Table 1**), and, as expected, their pharmacological inhibition could suppress OEA-induced sebaceous lipogenesis (**Figure 4e**). Furthermore, it should also be noted that Akt/PKB can phosphorylate and thereby inactivate glycogen synthase kinase-3α/β (GSK-3α/β), which leads to reduced ubiquitination and degradation of β-catenin (Beurel et al. 2015; Patel and Woodgett 2017; Souder and Anderson 2019). Of great importance, our data obtained by the phosphokinase array are completely in line with this. Indeed, we found that OEA-treatment led to the (inhibitory) S21/S9 phosphorylation of GSK-3α/β and to the elevation of β-catenin level (**Table 1**). Thus, these data indirectly argue that Akt/PKB is indeed activated upon OEA-treatment in human sebocytes.

Intriguingly, however, according to our pilot data obtained by the comparison of GPR119 expression in 6 acne and 6 acne-free patients, GPR119 was down-regulated in sebaceous glands of acne patients (**Figure 5a-c**). Although because of the relatively low number of involved patients, as well as of the apparent inter-donor variability, it would be premature to draw bold conclusions, our data argue that GPR119 signaling may indeed be disturbed at least in a subset of acne patients. Importantly, activation-induced down-regulation/desensitization is a commonly known phenomenon in case of several G-protein coupled receptors (Abdullah et al. 2016; Billington and Penn 2003; Geppetti et al. 2015; Skieterska et al. 2017), including GPR119 (Hassing et al. 2016; Zhang et al.

2014). Thus, our data highlight the possibility that GPR119 (over)activation might be involved in the initiation phase rather than later stages of acne. Alternatively, it is also possible that down-regulation of the pro-lipogenic GPR119 receptor is a secondary compensatory mechanism, and represents a biological response to the already highly elevated, acnegenic sebum production.

It is also important to note that the OEA concentrations used in this study may seem high in light of its usual plasma concentration (~4 nM) (Bachkangi et al. 2019). However, several lines of evidence argue that they are relevant. First, sebocytes express NAPE-PLD (i.e. a key enzyme involved in the synthesis of OEA (Igarashi et al. 2019)), therefore the local concentration of OEA may be higher than its serum level (Zákány et al. 2018). Second, according to the IUPHAR database, pEC_{50} value for OEA in case of GPR119 is 5.4–6.3 (i.e. ~500 nM–4 μM) (Alexander et al. 2019), which means that in order to fully activate GPR119, OEA definitely needs to be applied at the low micromolar range. Importantly, similar EC_{50} data (85 nM to 15 μM) were recently reported by Hassing et al. (Hassing et al. 2016), further underscoring the relevance of administering OEA at the micromolar range. Likewise, in another recent study, the authors used 5 mM 2-oleoylglycerol (2-OG) to activate GPR119, and to lower the intraocular pressure. According to their data obtained in $GPR119^{-/-}$ mice, the effects of this extremely high concentration of 2-OG were still mediated by GPR119 (Miller et al. 2017). This, together with the fact that pEC_{50} of 2-OG is 5.6 according to the IUPHAR database, i.e. it is almost identical to the one of OEA, collectively argue that administration of 50 μM OEA can be justified. Moreover, one should also take into consideration that sebocytes were cultured in a serum containing medium, and hence,

plasma proteins of the medium certainly bind some fraction of OEA. Therefore, it is highly likely that the concentration of the active, free fraction of this lipophilic molecule was less than the ones administered. Finally, it should also be noted that "classical" eCBs (i.e. AEA and 2-AG) also promoted sebaceous lipogenesis and differentiation at the low micromolar range (i.e. at 30 μM) in a receptor-dependent manner (Dobrosi et al. 2008).

Collectively, our findings introduce the OEA→GPR119 signaling pathway as a previously unidentified, positive regulator of human sebaceous lipogenesis and sebocyte differentiation. Since beyond these effects, administration of OEA led to a pro-inflammatory phenotype too, our data highlighted the possibility that dysregulation of the above signaling pathway may contribute to the development of acne, a disease characterized by increased sebaceous lipogenesis and inflammation (Zouboulis et al. 2014). Further studies are therefore invited to explore if disturbed OEA and/or GPR119 signaling play any role in seborrhea and/or acne, and if pharmacological blockade of GPR119 results in beneficial effects in these diseases. Finally, our data also warn of risk of potential cutaneous side effects (i.e. seborrhea and acne) upon clinical administration of GPR119 activators (further discussion of this potential issue can be found in the **Supplementary Discussion**).

MATERIALS & METHODS

Materials

Oleoylethanolamide (OEA), arachidonoylethanolamine (anandamide [AEA]), as well as the STAT5-inhibitor (2-[(4-oxo-4H-1-benzopyran-3-yl)methylene]hydrazide 3-pyridinecarboxylic acid; [$STAT5_i$]) were purchased from Cayman Chemical Company (Ann Arbor, MI, USA); γ-irradiated lipopolysaccharide from *Escherichia coli* 026:B6 (LPS), arachidonic acid (AA), linoleic acid (LA), and testosterone (T) were obtained from Sigma-Aldrich (St. Louis, MO, USA), PD 98059 (ERK1/2 MAPK-inhibitor (Qi et al. 2004)) from Calbiochem (Darmstadt, Germany), whereas SU 3327 (JNK-inhibitor (De et al. 2009)), GSK 690693 (Akt/PKB-inhibitor (Heerding et al. 2008)), compound 666-15 (CREB-inhibitor (Xie et al. 2015)), and GW 6471 (PPARα-antagonist (Müller et al. 2009)) from Tocris (Bio-Techne R&D Systems, Minneapolis, MN, USA). OEA, AEA, LA, and AA were dissolved in absolute ethanol, whereas the solvent for PD 98059, SU 3327, GSK 690693, compound 666-15, $STAT5_i$, and T was dimethyl sulfoxide (DMSO). LPS was dissolved in filtered distilled water.

Cell Culturing

Human immortalized SZ95 sebocytes, originated from human facial sebaceous glands (Zouboulis et al., 1999), were cultured in Sebomed® Basal Medium (Biochrom, Berlin, Germany) supplemented with 10 (V/V)% fetal bovine serum (Gibco, ThermoFisher, Waltham, Massachusetts, USA), 1 mM $CaCl_2$, 5 ng/ml human epidermal growth factor (Sigma-Aldrich), and MycoZap™ Plus-CL (1:500; Lonza, Basel, Switzerland). The medium was changed every other day, and cells were subcultured at 60-70% confluence. Cells were regularly checked for *Mycoplasma* contamination by using

MycoAlert™ PLUS Mycoplasma Detection Kit (Lonza), and every assessment yielded negative result.

Ethical approval

Primary human material was collected after obtaining written informed consent, adhering to Helsinki Declaration, and after obtaining Institutional Research Ethics Committee's and Government Office for Hajdú-Bihar County's permission (document IDs: IX-R-052/01396-2/2012, IF-12817/2015, IF-1647/2016, IF-778-5/2017, DE RKEB/IKEB 4988-2018).

Detailed description of the methods to assess sebaceous lipogenesis (Nile Red), differentiation-associated granulation (flow cytometry), viability (MTT-assay), cell death ($DilC_1(5)$-SYTOX Green labeling), proliferation (CyQUANT-assay), Ca^{2+}-homeostasis (Fluo-4 AM-based fluorescent Ca^{2+}-measurement), gene expression at the mRNA (Q-PCR) and protein levels (Western blot, immunohistochemistry, ELISA), and siRNA-mediated silencing can be found in our previous publications (Lisztes et al. 2019; Markovics et al. 2019; Oláh et al. 2017a; Oláh et al. 2016a; Oláh et al. 2014; Ramot et al. 2018; Szabó et al. 2020) and in the **Supplementary Materials & Methods**.

ORCID

Arnold Markovics: 0000-0001-5460-6380

Ágnes Angyal: 0000-0002-7386-7591

Kinga Fanni Tóth: 0000-0002-5184-8082

Dorottya Ádám: 0000-0002-3543-4146

Zsófia Pénzes: 0000-0002-3566-8532

József Magi: 0000-0002-3397-3592

Ágnes Pór: -

Ilona Kovács: -

Dániel Törőcsik: 0000-0002-6094-6266

Christos C. Zouboulis: 0000-0003-1646-2608

Tamás Bíró: 0000-0002-3770-6221

Attila Oláh: 0000-0003-4122-5639

CONFLICT OF INTEREST

CCZ owns an international patent on the SZ95 sebaceous gland cell line (WO2000046353). A.O. and T.B. provide consultancy services to Botanix Pharmaceuticals Ltd. (A.O.) and Phytecs Inc. as well as Monasterium Laboratory Skin & Hair Research Solutions GmbH (T.B.). Botanix Pharmaceuticals Ltd., Phytecs Inc., Monasterium Laboratory Skin & Hair Research Solutions GmbH, and the founding sponsors listed in the Acknowledgements section had no role in conceiving the study, designing the experiments, writing of the manuscript, or in the decision to publish it.

AUTHOR CONTRIBUTION ACCORDING TO CREDIT TAXONOMY

Conceptualization: TB, AO

Investigation: AM, ÁA, KFT, DÁ, ZsP, JM, ÁP, IK, DT, CCZ

Formal analysis: AM, ÁA, KFT

Funding acquisition: TB, AO

Project administration: AM, ÁA, KFT, DÁ, ZsP, JM, ÁP, IK, DT, CCZ

Provision: TB, AO

Supervision: TB, AO

Validation: AM, ÁA, KFT

Visualization: AM, ÁA, KFT

Writing – original draft: AM, ÁA, AO

Writing – review & editing: AM, ÁA, KFT, DÁ, ZsP, JM, ÁP, IK, DT, CCZ, TB, AO

ACKNOWLEDGEMENTS

This project was supported by Hungarian (NRDIO 120552, 121360, 125055, and GINOP-2.3.2-15-2016-00050) research grants. AO and DT were awarded by the *János Bolyai Research Scholarship* of the Hungarian Academy of Sciences, and AO is recipient of the "*Acne and rosacea basic research award 2015*" of Galderma International. AO's, DT's, and KFT's work was supported by the ÚNKP-19-4-DE-287 (AO), ÚNKP-19-4-DE-15 (DT), and ÚNKP-19-3-I-DE-141 (KFT) New National Excellence Program of the Ministry for Innovation and Technology. The authors are grateful to Anita Galicz for the excellent technical assistance.

DATA AVAILABILITY STATEMENT

The data that support the findings of this study are available from the corresponding author upon reasonable request.

REFERENCES

Abdullah N, Beg M, Soares D, Dittman JS, McGraw TE. Downregulation of a GPCR by β-Arrestin2-Mediated Switch from an Endosomal to a TGN Recycling Pathway. Cell Rep. 2016;17(11):2966–78

Alexander S. GPR18, GPR55 and GPR119: GPR119 [Internet]. IUPHARBPS Guide Pharmacol. 2016 [cited 2018 Apr 12]. Available from: http://www.guidetopharmacology.org/GRAC/ObjectDisplayForward?objectId=126&familyId=114&familyType=GPCR

Alexander SPH, Battey J, Benson HE, Benya RV, Bonner TI, Davenport AP, et al. Class A Orphans (version 2019.5) in the IUPHAR/BPS Guide to Pharmacology Database [Internet]. IUPHARBPS Guide Pharmacol. CITE 20195 Nov 2019. 2019 [cited 2020 Jan 6]. Available from: https://www.guidetopharmacology.org/GRAC/ObjectDisplayForward?objectId=126

Arifin SA, Paternoster S, Carlessi R, Casari I, Ekberg JH, Maffucci T, et al. Oleoyl-lysophosphatidylinositol enhances glucagon-like peptide-1 secretion from enteroendocrine L-cells through GPR119. Biochim. Biophys. Acta Mol. Cell Biol. Lipids. 2018;1863(9):1132–41

Bachkangi P, Taylor AH, Bari M, Maccarrone M, Konje JC. Prediction of preterm labour from a single blood test: The role of the endocannabinoid system in predicting preterm birth in high-risk women. Eur. J. Obstet. Gynecol. Reprod. Biol. 2019;243:1–6

Beurel E, Grieco SF, Jope RS. Glycogen synthase kinase-3 (GSK3): regulation, actions, and diseases. Pharmacol. Ther. 2015;148:114–31

Billington CK, Penn RB. Signaling and regulation of G protein-coupled receptors in airway smooth muscle. Respir. Res. 2003;4(1):2

Bíró T, Tóth BI, Haskó G, Paus R, Pacher P. The endocannabinoid system of the skin in health and disease: novel perspectives and therapeutic opportunities. Trends Pharmacol. Sci. 2009;30(8):411–20

Calebiro D, Maiellaro I. cAMP signaling microdomains and their observation by optical methods. Front. Cell. Neurosci. 2014;8:350

Choi JJ, Park MY, Lee HJ, Yoon D-Y, Lim Y, Hyun JW, et al. TNF-α increases lipogenesis via JNK and PI3K/Akt pathways in SZ95 human sebocytes. J. Dermatol. Sci. 2012;65(3):179–88

De SK, Stebbins JL, Chen L-H, Riel-Mehan M, Machleidt T, Dahl R, et al. Design, synthesis, and structure-activity relationship of substrate competitive, selective, and in vivo active triazole and thiadiazole inhibitors of the c-Jun N-terminal kinase. J. Med. Chem. 2009;52(7):1943–52

Dobrosi N, Tóth BI, Nagy G, Dózsa A, Géczy T, Nagy L, et al. Endocannabinoids enhance lipid synthesis and apoptosis of human sebocytes via cannabinoid receptor-2-mediated signaling. FASEB J. Off. Publ. Fed. Am. Soc. Exp. Biol. 2008;22(10):3685–95

Du K, Montminy M. CREB is a regulatory target for the protein kinase Akt/PKB. J. Biol. Chem. 1998;273(49):32377–9

Fu J, Gaetani S, Oveisi F, Lo Verme J, Serrano A, Rodríguez De Fonseca F, et al. Oleylethanolamide regulates feeding and body weight through activation of the nuclear receptor PPAR-alpha. Nature. 2003;425(6953):90–3

Géczy T, Oláh A, Tóth BI, Czifra G, Szöllősi AG, Szabó T, et al. Protein Kinase C Isoforms Have Differential Roles in the Regulation of Human Sebocyte Biology. J. Invest. Dermatol. 2012;132(8):1988–97

Geppetti P, Veldhuis NA, Lieu T, Bunnett NW. G Protein-Coupled Receptors: Dynamic Machines for Signaling Pain and Itch. Neuron. 2015;88(4):635–49

Haskó J, Fazakas C, Molnár J, Nyúl-Tóth Á, Herman H, Hermenean A, et al. CB2 receptor activation inhibits melanoma cell transmigration through the blood-brain barrier. Int. J. Mol. Sci. 2014;15(5):8063–74

Hassing HA, Fares S, Larsen O, Pad H, Hauge M, Jones RM, et al. Biased signaling of lipids and allosteric actions of synthetic molecules for GPR119. Biochem. Pharmacol. 2016;119:66–75

Heerding DA, Rhodes N, Leber JD, Clark TJ, Keenan RM, Lafrance LV, et al. Identification of 4-(2-(4-amino-1,2,5-oxadiazol-3-yl)-1-ethyl-7-{[(3S)-3-piperidinylmethyl]oxy}-1H-imidazo[4,5-c]pyridin-4-yl)-2-methyl-3-butyn-2-ol (GSK690693), a novel inhibitor of AKT kinase. J. Med. Chem. 2008;51(18):5663–79

Igarashi M, Watanabe K, Tsuduki T, Kimura I, Kubota N. NAPE-PLD controls OEA synthesis and fat absorption by regulating lipoprotein synthesis in an in vitro model of intestinal epithelial cells. FASEB J. Off. Publ. Fed. Am. Soc. Exp. Biol. 2019;33(3):3167–79

Kwon HC, Kim TY, Lee CM, Lee KS, Lee KK. Active compound chrysophanol of Cassia tora seeds suppresses heat-induced lipogenesis via inactivation of JNK/p38 MAPK signaling in human sebocytes. Lipids Health Dis. 2019;18(1):135

Legrand JMD, Roy E, Ellis JJ, Francois M, Brooks AJ, Khosrotehrani K. STAT5 Activation in the Dermal Papilla Is Important for Hair Follicle Growth Phase Induction. J. Invest. Dermatol. 2016;136(9):1781–91

Lisztes E, Tóth BI, Bertolini M, Szabó IL, Zákány N, Oláh A, et al. Adenosine Promotes Human Hair Growth and Inhibits Catagen Transition In Vitro: Role of the Outer Root Sheath Keratinocytes. J. Invest. Dermatol. 2019;

Maccarrone M, Bab I, Bíró T, Cabral GA, Dey SK, Di Marzo V, et al. Endocannabinoid signaling at the periphery: 50 years after THC. Trends Pharmacol. Sci. 2015;36(5):277–96

Makrantonaki E, Zouboulis CC. Testosterone metabolism to 5alpha-dihydrotestosterone and synthesis of sebaceous lipids is regulated by the peroxisome proliferator-activated receptor ligand linoleic acid in human sebocytes. Br. J. Dermatol. 2007;156(3):428–32

Markovics A, Tóth KF, Sós KE, Magi J, Gyöngyösi A, Benyó Z, et al. Nicotinic acid suppresses sebaceous lipogenesis of human sebocytes via activating hydroxycarboxylic acid receptor 2 (HCA2). J. Cell. Mol. Med. 2019;23(9):6203–14

Miller S, Hu SS-J, Leishman E, Morgan D, Wager-Miller J, Mackie K, et al. A GPR119 Signaling System in the Murine Eye Regulates Intraocular Pressure in a Sex-Dependent Manner. Invest. Ophthalmol. Vis. Sci. 2017;58(7):2930–8

Müller MQ, de Koning LJ, Schmidt A, Ihling C, Syha Y, Rau O, et al. An innovative method to study target protein-drug interactions by mass spectrometry. J. Med. Chem. 2009;52(9):2875–9

Oláh A, Ambrus L, Nicolussi S, Gertsch J, Tubak V, Kemény L, et al. Inhibition of fatty acid amide hydrolase exerts cutaneous anti-inflammatory effects both in vitro and in vivo. Exp. Dermatol. 2016a;25(4):328–30

Oláh A, Bíró T. Targeting Cutaneous Cannabinoid Signaling in Inflammation - A "High"-way to Heal? EBioMedicine. 2017;16:3–5

Oláh A, Markovics A, Szabó-Papp J, Szabó PT, Stott C, Zouboulis CC, et al. Differential effectiveness of selected non-psychotropic phytocannabinoids on human sebocyte functions implicates their introduction in dry/seborrhoeic skin and acne treatment. Exp. Dermatol. 2016b;25(9):701–7

Oláh A, Szabó-Papp J, Soeberdt M, Knie U, Dähnhardt-Pfeiffer S, Abels C, et al. Echinacea purpurea-derived alkylamides exhibit potent anti-inflammatory effects and alleviate clinical symptoms of atopic eczema. J. Dermatol. Sci. 2017a;88(1):67–77

Oláh A, Szekanecz Z, Bíró T. Targeting Cannabinoid Signaling in the Immune System: "High"-ly Exciting Questions, Possibilities, and Challenges. Front. Immunol. 2017b;8:1487

Oláh A, Tóth BI, Borbíró I, Sugawara K, Szöllõsi AG, Czifra G, et al. Cannabidiol exerts sebostatic and antiinflammatory effects on human sebocytes. J. Clin. Invest. 2014;124(9):3713–24

Patel P, Woodgett JR. Glycogen Synthase Kinase 3: A Kinase for All Pathways? Curr. Top. Dev. Biol. 2017;123:277–302

Pouysségur J. Signal transduction. An arresting start for MAPK. Science. 2000;290(5496):1515–8

Qi X, Li T-G, Hao J, Hu J, Wang J, Simmons H, et al. BMP4 supports self-renewal of embryonic stem cells by inhibiting mitogen-activated protein kinase pathways. Proc. Natl. Acad. Sci. U. S. A. 2004;101(16):6027–32

Qin Y, Verdegaal EME, Siderius M, Bebelman JP, Smit MJ, Leurs R, et al. Quantitative expression profiling of G-protein-coupled receptors (GPCRs) in metastatic melanoma: the constitutively active orphan GPCR GPR18 as novel drug target. Pigment Cell Melanoma Res. 2011;24(1):207–18

Ramot Y, Alam M, Oláh A, Bíró T, Ponce L, Chéret J, et al. Peroxisome Proliferator-Activated Receptor-γ-Mediated Signaling Regulates Mitochondrial Energy Metabolism in Human Hair Follicle Epithelium. J. Invest. Dermatol. 2018;

Scott GA, Jacobs SE, Pentland AP. sPLA2-X stimulates cutaneous melanocyte dendricity and pigmentation through a lysophosphatidylcholine-dependent mechanism. J. Invest. Dermatol. 2006;126(4):855–61

Skieterska K, Rondou P, Van Craenenbroeck K. Regulation of G Protein-Coupled Receptors by Ubiquitination. Int. J. Mol. Sci. 2017;18(5) Available from: https://www.ncbi.nlm.nih.gov/pmc/articles/PMC5454836/

Smith TM, Gilliland K, Clawson GA, Thiboutot D. IGF-1 induces SREBP-1 expression and lipogenesis in SEB-1 sebocytes via activation of the phosphoinositide 3-kinase/Akt pathway. J. Invest. Dermatol. 2008;128(5):1286–93

Solymosi K, Köfalvi A. Cannabis: A Treasure Trove or Pandora's Box? Mini Rev. Med. Chem. 2017;17(13):1223–91

Souder DC, Anderson RM. An expanding GSK3 network: implications for aging research. GeroScience. 2019;41(4):369–82

Szabó IL, Lisztes E, Béke G, Tóth KF, Paus R, Oláh A, et al. The Phytocannabinoid (-)-Cannabidiol Operates as a Complex, Differential Modulator of Human Hair Growth: Anti-Inflammatory Submicromolar versus Hair Growth Inhibitory Micromolar Effects. J. Invest. Dermatol. 2020;140(2):484-488.e5

Szántó M, Oláh A, Szöllősi AG, Tóth KF, Páyer E, Czakó N, et al. Activation of TRPV3 inhibits lipogenesis and stimulates production of inflammatory mediators in human sebocytes - a putative contributor to dry skin dermatoses. J. Invest. Dermatol. 2019;139(1):250–3

Szöllősi AG, Oláh A, Bíró T, Tóth BI. Recent advances in the endocrinology of the sebaceous gland. Dermatoendocrinol. 2017;0(ja):00–00

Törőcsik D, Kovács D, Camera E, Lovászi M, Cseri K, Nagy GG, et al. Leptin promotes a proinflammatory lipid profile and induces inflammatory pathways in human SZ95 sebocytes. Br. J. Dermatol. 2014;171(6):1326–35

Tóth KF, Ádám D, Bíró T, Oláh A. Cannabinoid Signaling in the Skin: Therapeutic Potential of the "C(ut)annabinoid" System. Mol. Basel Switz. 2019;24(5)

Tóth BI, Géczy T, Griger Z, Dózsa A, Seltmann H, Kovács L, et al. Transient receptor potential vanilloid-1 signaling as a regulator of human sebocyte biology. J. Invest. Dermatol. 2009;129(2):329–39

Tóth BI, Oláh A, Szöllősi AG, Czifra G, Bíró T. "Sebocytes' makeup" - Novel mechanisms and concepts in the physiology of the human sebaceous glands. Pflüg. Arch. - Eur. J. Physiol. 2011;461(6):593–606

Tyurenkov IN, Kurkin DV, Bakulin DA, Volotova EV, Chafeev MA, Smirnov AV, et al. ZB-16, a Novel GPR119 Agonist, Relieves the Severity of Streptozotocin-Nicotinamide-Induced Diabetes in Rats. Front. Endocrinol. 2017;8:152

Xie F, Li BX, Kassenbrock A, Xue C, Wang X, Qian DZ, et al. Identification of a Potent Inhibitor of CREB-Mediated Gene Transcription with Efficacious in Vivo Anticancer Activity. J. Med. Chem. 2015;58(12):5075–87

Zákány N, Oláh A, Markovics A, Takács E, Aranyász A, Nicolussi S, et al. Endocannabinoid Tone Regulates Human Sebocyte Biology. J. Invest. Dermatol. 2018;138(8):1699–706

Zhang S, Li J, Xie X. Discovery and characterization of novel smallmolecule agonists of G protein-coupled receptor 119. Acta Pharmacol. Sin. 2014;35(4):540–8

Zouboulis CC, Katsambas AD, Kligman AM. Pathogenesis and Treatment of Acne and Rosacea. Springer; 2014.

Zouboulis CC, Schagen S, Alestas T. The sebocyte culture: a model to study the pathophysiology of the sebaceous gland in sebostasis, seborrhoea and acne. Arch. Dermatol. Res. 2008;300(8):397–413

Zouboulis CC, Seltmann H, Orfanos CE, Neitzel H. Establishment and Characterization of an Immortalized Human Sebaceous Gland Cell Line (SZ95)1. J. Invest. Dermatol. 1999;113(6):1011–20

Table 1 *List of signaling molecules exhibiting relevant (≥1.3-fold) increase in phosphokinase array signal intensity following 20 min treatment with 50 μM OEA*

Signaling molecule		Phosphorylation site	Fold-change over vehicle control
Abbreviation	**Full name**		
JNK 1/2/3	c-Jun N-terminal kinase 1/2/3	T183/Y185 (activating phosphorylation of JNK1 and 2), T221/Y223 (activating phosphorylation of JNK3)	1.31
AMPKα1	AMP-activated protein kinase α1	T183 (activating phosphorylation)	1.36
CREB	cAMP responsive element binding protein 1	S133 (activating phosphorylation)	1.37
STAT5b	Signal transducer and activator of transcription 5b	Y699 (activating phosphorylation)	1.39
STAT5a	Signal transducer and activator of transcription 5a	Y694 (activating phosphorylation)	1.40
GSK-3α/β	Glycogen synthase kinase-3α/β	S21/S9 (**inhibitory** phosphorylation)	1.41
STAT5a/b	Signal transducer and activator of transcription 5a/b	Y694/Y699 (activating phosphorylation)	1.42
AKT 1/2/3	Protein kinase B	S473 (activating phosphorylation)	1.46
-	β-Catenin	-	1.57

FIGURE LEGENDS

Figure 1 *The GPR119 agonist OEA promotes sebaceous lipogenesis and induces differentiation of human sebocytes*

(**a-b** and **d**) Nile Red assays. Lipogenesis of SZ95 sebocytes was assessed following 24- (**a**) and 48-hr (**b** and **d**) treatments. Results are expressed in the percentage of the vehicle control (100%, solid line) as mean±SEM of four independent determinations. Two additional experiments yielded similar results. *, **, and *** mark significant (P<0.05, 0.01, and 0.001, respectively) differences compared to the respective vehicle treated control group. (**c**) Flow cytometry. Sebocytes were treated as indicated for 48 hrs, and granularity was then measured by assessing side scatter. Right shift of the curve indicates increased granulation upon OEA treatment. (**e**) Combined fluorescent $DilC_1(5)$-SYTOX Green labeling. To monitor apoptotic and necrotic cell death, SZ95 sebocytes were treated as indicated for 48 hours. Results are expressed in the percentage of the vehicle control (100%, solid line; $DilC_1(5)$, apoptosis data) or in the percentage of the positive control (100%, solid line; SYTOX Green, necrosis data) as mean±SEM of four independent determinations. Two additional experiments yielded similar results. ** and *** mark significant (P<0.01 or P<0.001) differences compared to the respective ($DilC_1(5)$ or SYTOX Green) vehicle control groups. **CCCP:** carbonyl cyanide m-chlorophenyl hydrazone (1:200; apoptosis positive control); **LB:** lysis buffer (1:100; positive control for necrosis); **AA:** arachidonic acid (50 μM); **AEA:** anandamide (30 μM); **LA+T:** linoleic acid (100 μM) + testosterone (1 μM); **OEA:** oleoylethanolamide.

Figure 2 *OEA increases expression and release of several pro-inflammatory cytokines*

(**a-d**) Q-PCR. *IL-1α*, *IL-1β*, *IL-6*, and *IL-8* mRNA expression in human SZ95 sebocytes was determined following the indicated 3-hr treatments. Data are presented by using ΔΔCT method regarding *18S RNA*-normalized mRNA expressions of the vehicle control as 1. Data are expressed as mean±SD of 3 determinations. One additional experiment yielded similar results. ***P<0.001 compared to the control group. (**e**-**f**) ELISA. IL-6 and IL-8 content of the sebocyte supernatants was determined following the indicated 3-hr treatments. Data are expressed as mean±SEM of 2-3 determinations. One additional experiment yielded similar results. *, and *** mark significant (P<0.05, or 0.001, respectively) differences compared to the control group. **LPS:** lipopolysaccharide; **OEA:** oleoylethanolamide.

Figure 3 *Lipogenic effect of OEA is mediated via activation of GPR119, and is independent of PPARα*

(**a**) Nile Red assay. Lipogenesis of SZ95 sebocytes was assessed following 48-hr treatments. Results are expressed in the percentage of the vehicle control (100%, solid line) as mean±SEM of four independent determinations. Two additional experiments yielded similar results. *** marks significant (P<0.001) difference as indicated. n.s.: not significant. (**b**) Q-PCR. SZ95 sebocytes were harvested at different confluences. GPR119 expression was normalized to the level of glyceraldehyde-3-phosphate dehydrogenase (GAPDH) of the same sample, and is expressed as mean±SD of three determinations. (**c**) Pre- and post-confluent sebocytes were harvested, and cell lysate was subjected to Western blot analysis to detect GPR119 expression at the protein level. (**d**) Immunohistochemistry. Specific immunopositivity was visualized by 3,3'-

diaminobenzidine (DAB; brown color), whereas nuclei were counterstained by hematoxylin (blue color). Original magnification: 400x; scale bars: 50 μm. Negative control (bottom) was obtained by omitting the primary antibody. (**e**) GPR119 mRNA expression was down-regulated by GPR119 siRNA transfection (siGPR119). SZ95 sebocytes were harvested on post-transfection day 2. GPR119 expression was detected by Q-PCR. GPR119 expression was first normalized to the expression level of *18S RNA* of the same sample used as internal control, and relative mRNA expression was then normalized to the one of the non-sense RNA transfected scrambled (SCR) control group. Data are expressed as mean±SD of three determinations. (**f**) Western blot analyses of lysates of non-sense RNA transfected (**SCR:** scrambled control), and GPR119-silenced SZ95 sebocytes harvested on post-transfection Day 2. (**g**) Sebaceous lipogenesis assessed by Nile Red assay on SCR-transfected as well as GPR119-silenced sebocytes. 48-hr treatments were initiated on post-transfection Day 3. Results are expressed in the percentage of the SCR vehicle control (100%, solid line) as mean±SEM of four independent determinations. Two additional experiments yielded similar results.

Figure 4 *Lipogenic action of OEA is mediated via activating ERK1/2, JNK, and CREB, but is likely to be independent of STAT5*

(**a**) Western blot analysis of lysates of SZ95 sebocytes treated with OEA or vehicle for 20 minutes. Two additional experiments yielded similar results. (**b**) Sebaceous lipogenesis assessed by Nile Red assay following the indicated 24-hr treatments. Results are expressed in the percentage of the vehicle control (100%, solid line) as mean±SEM of twelve independent determinations. (**c**) cAMP ELISA. Sebocytes were

treated for 60 min with OEA or vehicle. Data are presented as mean±SD of three determinations. n.s.: not significant, as indicated. (**d-e**) Nile Red assays. Lipogenesis of SZ95 sebocytes was assessed following 48-hr treatments. Results are expressed in the percentage of the vehicle control (100%, solid line) as mean±SEM of eight (**d**) or twelve (**e**) independent determinations. *** marks significant (P<0.001) difference as indicated. n.s.: not significant. **666-15:** CREB-inhibitor; **GSK 690693:** Akt/PKB-inhibitor; **OD:** normalized optical densities (control = 1). **OEA:** oleoylethanolamide; **PD 89059:** ERK1/2 MAPK inhibitor; **STAT5$_i$:** STAT5-inhibitor; **SU 3327:** JNK-inhibitor.

Figure 5 *GPR119 is down-regulated in sebaceous glands of acne patients*

(**a-b**) Representative immunohistochemistry images. Specific immunopositivity was visualized by 3,3'-diaminobenzidine (DAB; brown color), whereas nuclei were counterstained by hematoxylin (blue color). Original magnification: 200x; scale bars: 100 μm. (**c**) Statistical analysis of GPR119 signal intensity obtained by semi-quantitative image analysis (scatter plot superimposed with mean±SD of the donors). Each dot represents mean signal intensity of one control subject (blue) or one acne patient (red).

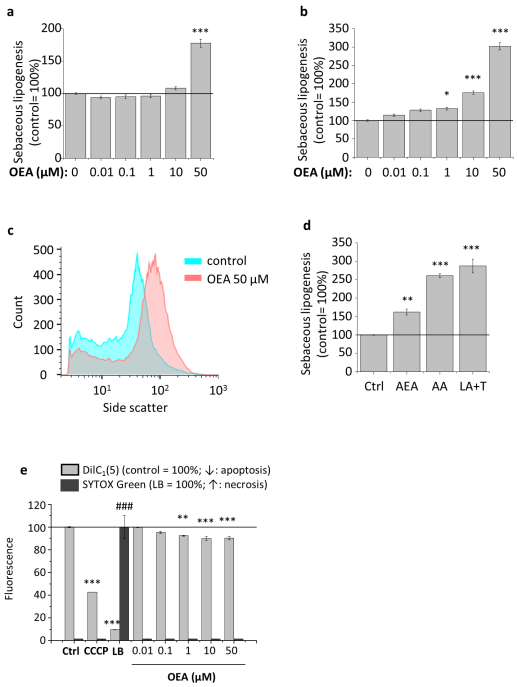
a
Sebaceous lipogenesis (control= 100%)
OEA (μM): 0 0.01 0.1 1 10 50
b
Sebaceous lipogenesis (control= 100%)
OEA (μM): 0 0.01 0.1 1 10 50
c
control
OEA 50 μM
Count
Side scatter
d
Sebaceous lipogenesis (control= 100%)
Ctrl AEA AA LA+T
e
DiIC1(5) (control = 100%; ↓: apoptosis)
SYTOX Green (LB = 100%; ↑: necrosis)
Fluorescence
Ctrl CCCP LB 0.01 0.1 1 10 50
OEA (μM)

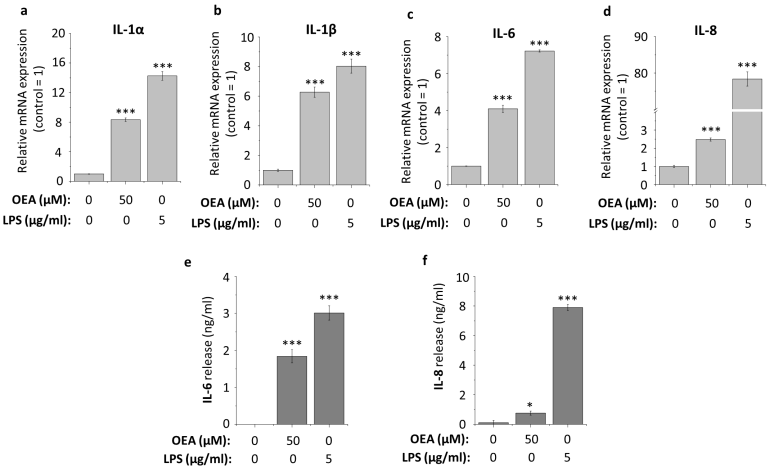
a
IL-1α
Relative mRNA expression (control = 1)
b
IL-1β
c
IL-6
d
IL-8
OEA (μM): 0 50 0
LPS (μg/ml): 0 0 5
***

e
IL-6 release (ng/ml)
f
IL-8 release (ng/ml)
OEA (μM): 0 50 0
LPS (μg/ml): 0 0 5
***
*

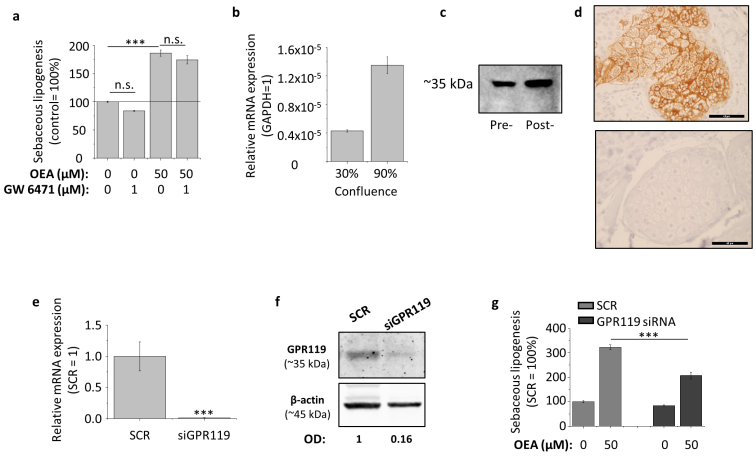
a
Sebaceous lipogenesis (control= 100%)
200
150
100
50
0
***
n.s.
n.s.
OEA (μM): 0 0 50 50
GW 6471 (μM): 0 1 0 1
b
Relative mRNA expression (GAPDH=1)
1.6x10-5
1.2x10-5
0.8x10-5
0.4x10-5
0
30% 90%
Confluence
c
~35 kDa
Pre- Post-
d
e
Relative mRNA expression (SCR = 1)
1.5
1.0
0.5
0.0
***
SCR siGPR119
f
SCR siGPR119
GPR119 (~35 kDa)
β-actin (~45 kDa)
OD: 1 0.16
g
SCR
GPR119 siRNA
Sebaceous lipogenesis (SCR = 100%)
400
300
200
100
0
***
OEA (μM): 0 50 0 50

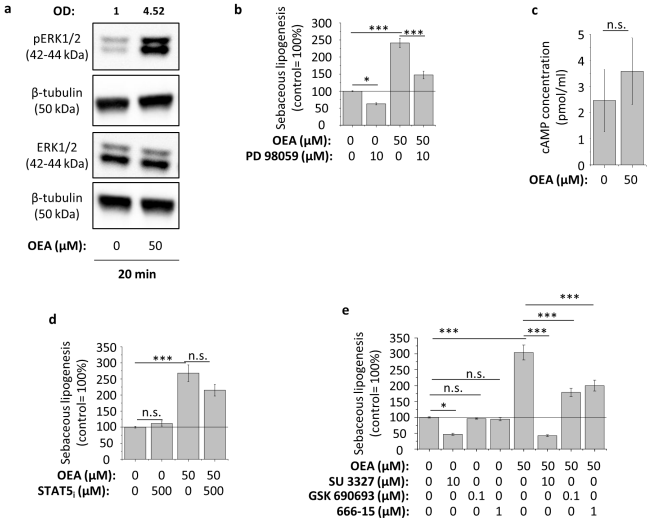
a
OD: 1 4.52
pERK1/2 (42-44 kDa)
β-tubulin (50 kDa)
ERK1/2 (42-44 kDa)
β-tubulin (50 kDa)
OEA (μM): 0 50
20 min
b
Sebaceous lipogenesis (control= 100%)
OEA (μM): 0 0 50 50
PD 98059 (μM): 0 10 0 10
c
cAMP concentration (pmol/ml)
n.s.
OEA (μM): 0 50
d
Sebaceous lipogenesis (control= 100%)
n.s.
OEA (μM): 0 0 50 50
STAT5i (μM): 0 500 0 500
e
Sebaceous lipogenesis (control= 100%)
OEA (μM): 0 0 0 0 50 50 50 50
SU 3327 (μM): 0 10 0 0 0 10 0 0
GSK 690693 (μM): 0 0 0.1 0 0 0 0.1 0
666-15 (μM): 0 0 0 1 0 0 0 1

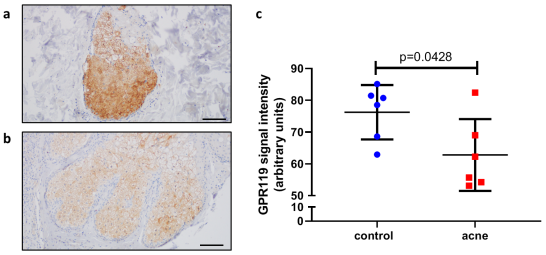
a
b
c
p=0.0428
GPR119 signal intensity (arbitrary units)
90
80
70
60
50
10
0
control
acne

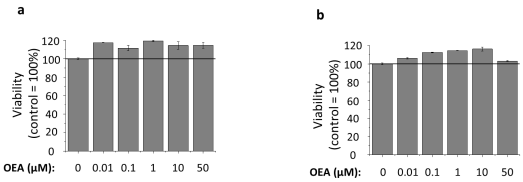
a
Viability
(control = 100%)
120
100
80
60
40
20
0
OEA (μM):
0
0.01
0.1
1
10
50
b
Viability
(control = 100%)
120
100
80
60
40
20
0
OEA (μM):
0
0.01
0.1
1
10
50

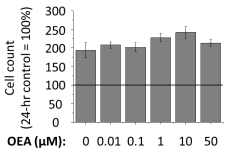
Cell count
(24-hr control = 100%)
300
250
200
150
100
50
0
OEA (μM): 0 0.01 0.1 1 10 50

a

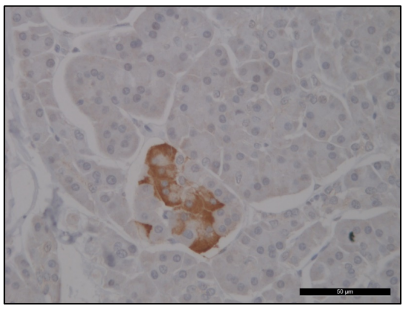

b

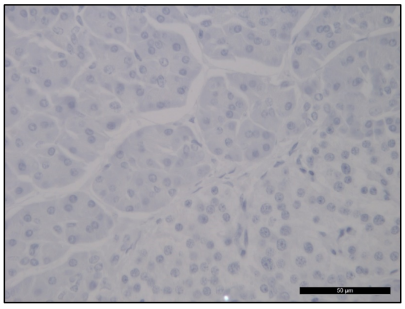

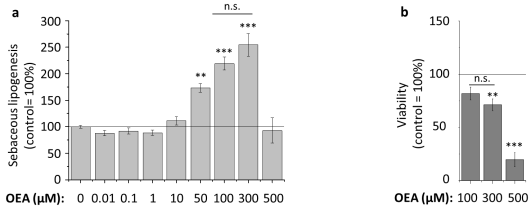
a
Sebaceous lipogenesis (control= 100%)
300
250
200
150
100
50
0
n.s.
***
***
**
OEA (μM): 0 0.01 0.1 1 10 50 100 300 500
b
Viability (control = 100%)
150
100
50
0
n.s.
**
***
OEA (μM): 100 300 500

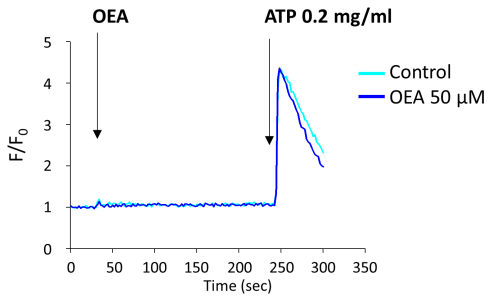
OEA
ATP 0.2 mg/ml
Control
OEA 50 µM
F/F0
0
1
2
3
4
5
0
50
100
150
200
250
300
350
Time (sec)

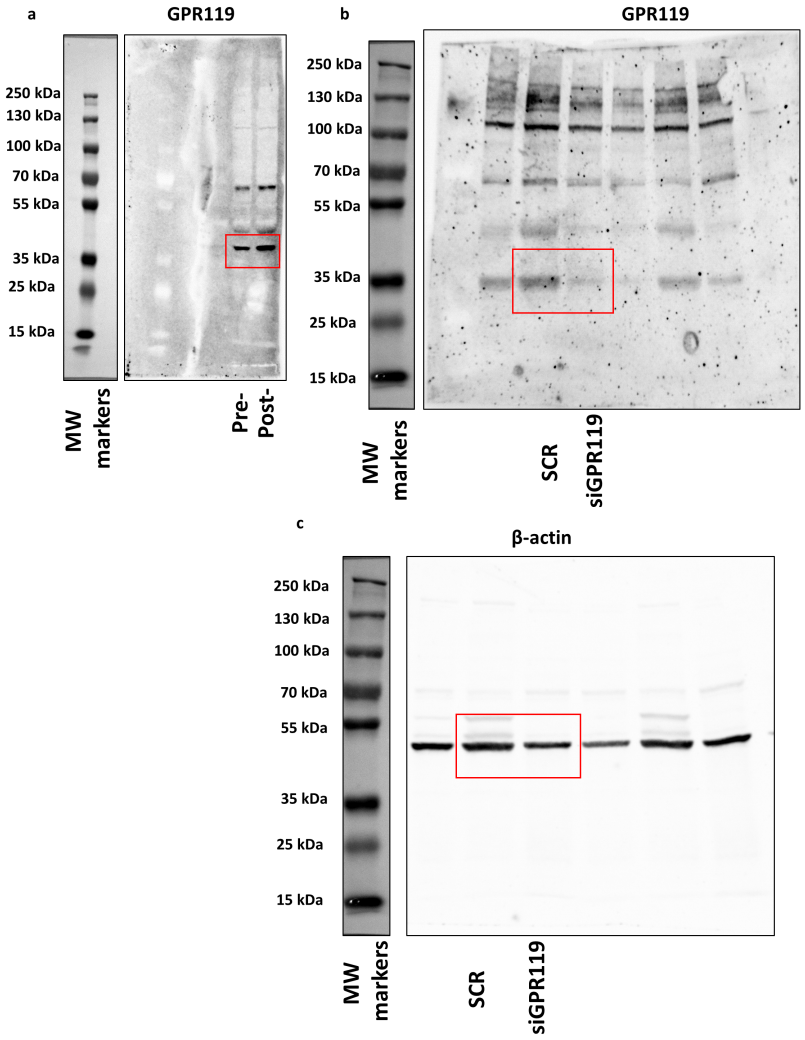
a
GPR119
250 kDa
130 kDa
100 kDa
70 kDa
55 kDa
35 kDa
25 kDa
15 kDa
MW markers
Pre-
Post-
b
GPR119
250 kDa
130 kDa
100 kDa
70 kDa
55 kDa
35 kDa
25 kDa
15 kDa
MW markers
SCR
siGPR119
c
β-actin
250 kDa
130 kDa
100 kDa
70 kDa
55 kDa
35 kDa
25 kDa
15 kDa
MW markers
SCR
siGPR119

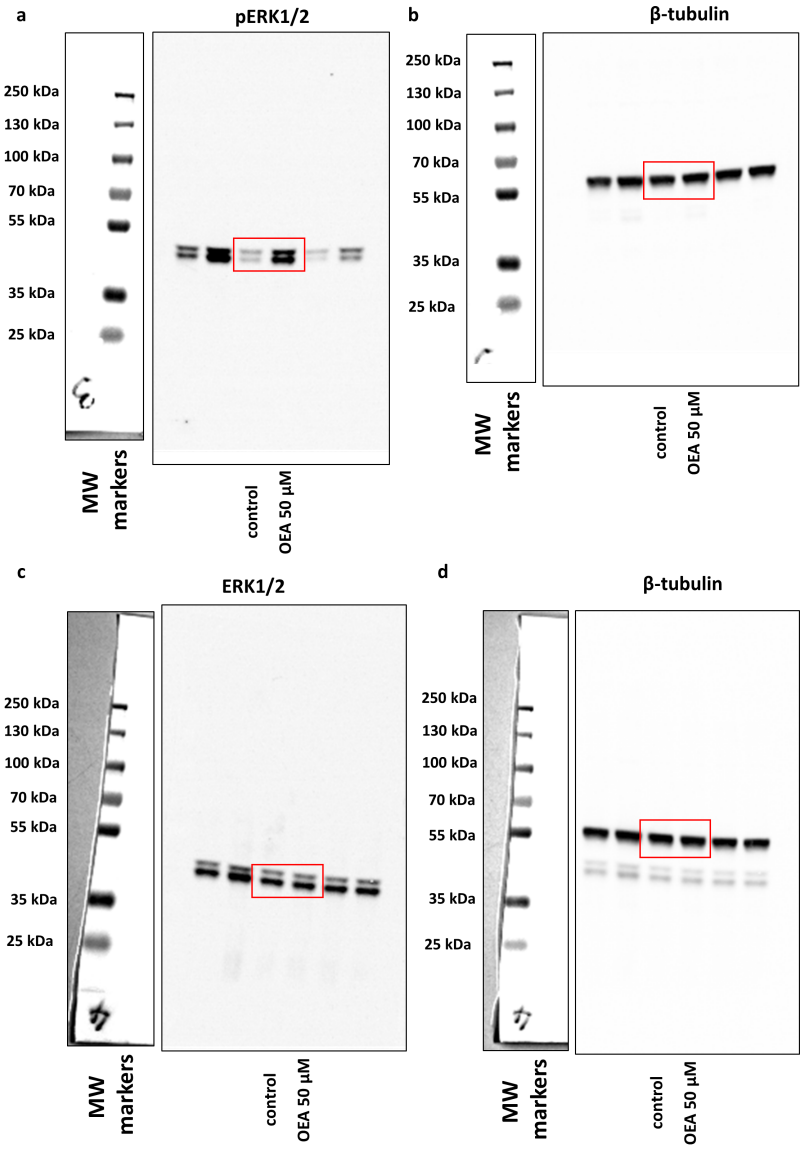
a
pERK1/2
250 kDa
130 kDa
100 kDa
70 kDa
55 kDa
35 kDa
25 kDa
MW markers
control
OEA 50 µM
b
β-tubulin
250 kDa
130 kDa
100 kDa
70 kDa
55 kDa
35 kDa
25 kDa
MW markers
control
OEA 50 µM
c
ERK1/2
250 kDa
130 kDa
100 kDa
70 kDa
55 kDa
35 kDa
25 kDa
MW markers
control
OEA 50 µM
d
β-tubulin
250 kDa
130 kDa
100 kDa
70 kDa
55 kDa
35 kDa
25 kDa
MW markers
control
OEA 50 µM

SUPPLEMENTARY MATERIALS & METHODS

Determination Of Intracellular Lipids

For quantitative measurement of sebaceous (neutral) lipid content, SZ95 sebocytes (20,000 cells/well) were cultured in 96-well "black well/clear bottom" plates (Greiner Bio-One, Frickenhausen, Germany) in quadruplicates, and were treated with compounds as indicated. Subsequently, supernatants were discarded, cells were washed twice with phosphate-buffered saline (PBS; 115 mM NaCl, 20 mM Na_2HPO_4, pH 7.4; all from Sigma-Aldrich), and 100 μl of a 1 μg/ml Nile Red (Sigma-Aldrich) solution in PBS was added to each well. The plates were then incubated at 37°C for 30 min, and fluorescence was measured on FlexStation 3 multimode microplate reader (Molecular Devices, San Francisco, CA, USA). Results, measured in relative fluorescence units, are expressed as percentage of the vehicle control regarded as 100%, using 485 nm excitation and 565 nm emission wavelengths.

Determination Of Cellular Viability

The viability of SZ95 sebocytes was determined by MTT-assay (Sigma-Aldrich) measuring the conversion of the tetrazolium salt to formazan by mitochondrial dehydrogenases. Cells were plated in 96-well plates (20,000 cells/well) in quadruplicates, and were treated as indicated. Cells were then incubated with 0.5 mg/ml MTT reagent for 3 hrs, and concentration of formazan crystals (as an indicator of number of viable cells) was determined colorimetrically at 565 nm by using FlexStation 3 multi-mode microplate reader (Molecular Devices). Results were expressed as percentage of vehicle control regarded as 100%.

Determination Of Apoptosis

A decrease in the mitochondrial membrane potential is one of the earliest markers of apoptosis (Green and Reed, 1998, Susin et al. 1998). Therefore, to assess the process, mitochondrial membrane potential of SZ95 sebocytes was determined using a MitoProbe™ $DilC_1(5)$ Assay Kit (Invitrogen/ThermoFisher). Cells (20,000 cells/well) were cultured in 96-well "black well/clear bottom" plates (Greiner Bio-One) in quadruplicates and were treated as indicated. After removal of supernatants, cells were incubated for 30 minutes with $DilC_1(5)$ working solution (50 µl/well), then washed with PBS, and the fluorescence of $DilC_1(5)$ was measured at 630 nm excitation and 670 nm emission wavelengths using FlexStation 3 multi-mode microplate reader (Molecular Devices). Relative fluorescence values were expressed as percentage of vehicle control regarded as 100%. As a positive control for apoptosis, we applied carbonyl cyanide m-chlorophenyl hydrazone (CCCP; Life Technologies Hungary Ltd.) dissolved in the $DilC_1(5)$ working solution (1:200 for 30 min at 37°C).

Determination Of Necrosis

Necrotic processes were determined by SYTOX Green staining (ThermoFisher). The dye is able to penetrate (and then to bind to the nucleic acids) only to necrotic cells with ruptured plasma membranes, whereas healthy cells with intact surface membranes show negligible SYTOX Green staining intensity. Cells were cultured in 96-well "black well/clear bottom" plates (Greiner Bio-One), and treated as indicated. Supernatants were then discarded, and SZ95 sebocytes were incubated for 30 minutes with 1 µM SYTOX Green dye. Following incubation, cells were washed with PBS, the culture medium was replaced, and fluorescence of SYTOX Green was measured at 490 nm

excitation and 520 nm emission wavelengths using FlexStation 3 multi-mode microplate reader (Molecular Devices). As a positive control for necrosis, lysis buffer (LB; 1:100 in the SYTOX Green working solution for 30 min at 37°C; Life Technologies Hungary Ltd.) was applied. Relative fluorescence values were expressed as percentage of positive control regarded as 100%. Due to their spectral properties, $DilC_1(5)$ and SYTOX Green dyes were always administered together, enabling us to investigate necrotic and early apoptotic processes of the same cultures. Selective decrease of $DilC_1(5)$ intensity indicated mitochondrial depolarization (i.e. the onset of early apoptotic processes), whereas increase of SYTOX Green staining intensity revealed necrotic cell death.

Determination Of Cellular Proliferation

The degree of cellular growth (reflecting proliferation) was determined by measuring the DNA content of cells using CyQUANT Cell Proliferation Assay Kit (Invitrogen/ThermoFisher). SZ95 sebocytes (2,000 cells per well) were cultured in 96-well "black well/clear bottom" plates (Greiner Bio-One) and were treated as indicated. Supernatants were then removed by blotting on paper towels, and the plates were subsequently frozen at -80°C. The plates were then thawed at room temperature, and 200 μl of CyQUANT dye/cell lysis buffer mixture was added to each well. After 5 min of incubation, fluorescence was measured at 490 nm excitation and 520 nm emission wavelengths using FlexStation 3 multimode microplate reader (Molecular Devices). Relative fluorescence values were expressed as percentage of 24-hr vehicle control regarded as 100%.

Flow Cytometry

SZ95 sebocytes were cultured in 6-well plates and treated with OEA or vehicle for 48 hrs. Then, cells were scraped in PBS, and the suspension was homogenized by intense trituration. Finally, the cells were subjected to flow cytometry in a BD FACS Calibur (Franklin Lakes, NJ, USA). As a parameter reflecting cellular granulation, and hence differentiation, side scatter was detected, and data were analyzed using *FlowJo* (FlowJo LLC, Ashland, OR, USA) software.

RNA Isolation, Reverse Transcription And Quantitative 'Real-Time' PCR (Q-PCR)

Q-PCR was performed on a Roche LightCycler 480 System (Roche, Basel, Switzerland) using the 5' nuclease assay. Total RNA was isolated using TRIzol (Sigma-Aldrich), DNase treatment was performed according to the manufacturer's protocol, and then, 1 μg of total RNA was reverse-transcribed into cDNA using High-Capacity cDNA Kit from Ambion™ (Invitrogen, ThermoFisher). PCR amplification was performed using the TaqMan® Gene Expression Assays (assay IDs: Hs00174092_m1 for *interleukin [IL]-1α*, Hs00174097_m1 for *IL-1β*, Hs00985639_m1 for *IL-6*, Hs00174103_m1 for *IL-8*, Hs02825719_s1 for *GPR119*) and the TaqMan universal PCR master mix protocol (Applied Biosystems). As internal controls, transcripts of *18S RNA* (assay ID: Hs03928985_g1) or *glyceraldehyde 3-phosphate dehydrogenase* (*GAPDH*; assay ID: Hs99999901_s1) were determined. The amount of the transcripts was normalized to those of the housekeeping gene using the ΔCT method. Finally, when indicated, the

relative expression values were further normalized to the ones of the vehicle-treated or scrambled RNA-transfected controls (ΔΔCT method).

Western Blotting

SZ95 sebocytes were harvested in lysis buffer (20 mM Tris-HCl, pH 7.4, 5 mM EGTA, 1 mM 4-(2-aminoethyl) benzensulfonyl fluoride, protease inhibitor cocktail diluted 1:100, and PhosSTOP (1 tablet/10 ml) (all from Sigma-Aldrich), and the protein content was measured by a modified BCA protein assay (Pierce, Rockford, IL, USA). The samples were then subjected to sodium dodecyl sulfate-polyacrylamide gel electrophoresis. 10% Mini Protean TGX gels (Bio-Rad, Hercules, CA, USA) were loaded with equal (10 μg) amount of protein per lane. Samples were then transferred to nitrocellulose membranes, by using Trans-Blot® Turbo™ Nitrocellulose Transfer Packs and Trans-Blot Turbo™ System (both from Bio-Rad), and then probed overnight with rabbit-anti-human GPR119 specific primary antibodies (Novus Biologicals, LLC, Littleton, Co, USA; cat. No. NBP1-00857; in 1:500 dilution in 5% milk containing TBST [50 mM Tris, 150 mM NaCl, pH 7.5; 0.1 V/V% Tween 20, all from Sigma-Aldrich]), rabbit-anti-human MAPK ERK1/2, as well as mouse-anti-human P-ERK1/2 (both from Santa Cruz; 1:20,000 [ERK1/2] and 1:10,000 [P-ERK1/2] dilution in both cases in 5% milk containing TBST; cat. No. m3682 and m8159, respectively). As secondary antibodies, horseradish peroxidase-conjugated, goat anti rabbit and mouse IgG Fc segment (both from Bio-Rad; 1:10000 in 5% milk containing TBST; cat. No. 170-6515 and 172-1011, respectively) were used, and the immunoreactive bands were visualized by a SuperSignal® West Pico Chemiluminescent Substrate enhanced chemiluminescence kit (Pierce) using a KODAK Gel Logic 1500 Imaging System

(Eastman Kodak Company, Kodak, Tokyo, Japan). To assess equal loading, membranes were re-probed with rabbit-anti-β-tubulin or rabbit-anti-β-actin antibodies (1:1000 dilution in 5% milk containing TBST in both cases; rabbit-anti-β-tubulin: Novus Biologicals, LLC; cat. No. NB600-936; rabbit-anti-β-actin: Sigma-Aldrich; cat. No. A5060), and visualized as described above. Semiquantitative densitometric analysis of the signals was performed by using *Fiji* software (National Institutes of Health, Bethesda, MD, USA). Full, uncut gels are presented on **Supplementary Figures 6** and **7**.

Phosphokinase Array

In order to simultaneously assess the involvement of several kinase cascades in mediating the cellular effects of OEA, Proteome Profiler Human Phospho-Kinase Array Kit (cat. No. ARY003B; Bio-Techne R&D Systems) was used according to the manufacturer's protocol. Briefly, SZ95 sebocytes were seeded to Petri dishes (d = 200 mm; 10 million cells/15 ml culture medium/Petri dish). On the other day, sebocytes were treated by 50 μM OEA or vehicle for 20 min. Next, the samples were harvested by using the lysis buffer provided as part of the kit, and their protein content was determined as described in the western blot section. Equal protein amounts (933 μg in 334 μl) were loaded, and the membranes were processed following the manufacturer's protocol, except that the immunoreactive spots were visualized by a SuperSignal® West Femto Chemiluminescent Substrate enhanced chemiluminescence kit (Pierce) using a KODAK Gel Logic 1500 Imaging System (Eastman Kodak Company, Kodak). Semiquantitative densitometric analysis of the signals was performed by using *Fiji* software (National Institutes of Health). Means of the negative control spots on each

membrane were considered as background signal intensities, and were subtracted from the raw values. Background subtracted values were then normalized to the respective control data, and ≥1.3-fold increase was considered to be relevant alteration (**Table 1**).

Immunohistochemistry

Primary human material was collected after obtaining written informed consent, adhering to Helsinki Declaration, and after obtaining Institutional Research Ethics Committee's and Government Office for Hajdú-Bihar County's permission (document IDs: IX-R-052/01396-2/2012, IF-12817/2015, IF-1647/2016, IF-778-5/2017, DE RKEB/IKEB 4988-2018).

The immunohistochemical investigation of GPR119 was performed on 3 formalin fixed paraffin embedded, skin samples rich in sebaceous glands, all diagnosed as trichilemmal cyst in Gyula Kenézy University Hospital (University of Debrecen). Serial 4 μm thick sections were cut from paraffin blocks, and heat-induced antigen retrieval was performed. GPR119 epitopes were retrieved in 11 mM citrate buffer (pH 6) applied in pressure cooker for 2 min on full pressure. Endogenous peroxidase activity was blocked with 3% H_2O_2 for 10 minutes. Next, tissue sections were incubated at room temperature with rabbit primary antibodies recognizing human GPR119 (Novus Biologicals; cat. No. NBP1-00857) diluted in 1% bovine serum albumin (1:500; 60 min at room temperature; Sigma-Aldrich, St. Louis, MO, USA). Sections were then incubated with the EnVision FLEX Labeled polymer-HRP anti-rabbit and anti-mouse System (DAKO, Glostrup, Denmark) at room temperature for 30 min with 3,3'-diaminobenzidine (DAB) visualization techniques. Cell nuclei were counterstained with hematoxylin and tissue sections were finally mounted in permanent mounting medium (Histolab, Göteborg, Sweden). As positive control, human pancreas (Sakamoto et al. 2006) was labeled (**Supplementary Figure S3**). Since the manufacturer could not provide appropriate

blocking peptide, negative controls were obtained by omitting the primary antibody in all cases.

Assessment Of The Putative Expressional Alterations Of GPR119 In Acne

Since the production of the above antibody has been discontinued, we optimized a second staining protocol with another antibody, which reproduced the expression pattern of the previously administered antibody (see **Figure 3d** and **Figure 5a**). Expression of GPR119 was assessed in skin samples of 6 acne-free patients (having pigmented nevi) as well as of 6 acne patients (relevant data of the donors can be found in **Supplementary Table S1**). Serial 4 μm thick sections were cut from paraffin blocks, and heat-induced antigen retrieval was performed. GPR119 epitopes were retrieved in 1 mM EDTA buffer (pH 8) applied in microwave oven for 15 min on 700W. Endogenous peroxidase activity was blocked with 3% H_2O_2 for 10 minutes. Next, tissue sections were incubated at room temperature with rabbit primary antibodies recognizing human GPR119 (Abcam, Cambridge, UK; cat. No. ab75312) diluted in 1% bovine serum albumin (1:100; 60 min at room temperature; Sigma-Aldrich, St. Louis, MO, USA). Sections were then incubated with the EnVision FLEX Labeled polymer-HRP anti-rabbit and anti-mouse System (DAKO, Glostrup, Denmark) at room temperature for 30 min with 3,3'-diaminobenzidine (DAB) visualization techniques. Cell nuclei were counterstained with hematoxylin and tissue sections were finally mounted in permanent mounting medium (Histolab, Göteborg, Sweden). Since the manufacturer could not provide appropriate blocking peptide, negative controls were obtained by omitting the primary antibody in all cases. Visualization of the labeling was performed by using Olympus Fluorescent Microscope (UNICAM Magyarország Ltd., Budapest, Hungary). Original magnification was 200x in all cases. Semi-quantitative image analysis was performed by using *ImageJ 1.49v* software (National Institute of Health, Bethesda, MD, USA).

Determination Of Cytokine Release (ELISA)

Cells were treated as indicated for 3 hrs. Supernatants were collected, and the released amount of IL-6 and IL-8 cytokines was determined using OptEIA kits (BD Biosciences, San Diego, USA) according to the manufacturer's protocol.

Fluorescent Ca^{2+} Measurements

Human SZ95 sebocytes were seeded in 96-well "black well/clear bottom" plates (Greiner Bio-One) at a density of 20,000 cells per well. The cells were washed once with 1% bovine serum albumin and 2.5 mM probenecid (both from Sigma-Aldrich) containing Hank's solution (136.8 mM NaCl, 5.4 mM KCl, 0.34 mM Na_2HPO_4, 0.44 mM KH_2PO_4, 0.81 mM $MgSO_4$, 1.26 mM $CaCl_2$, 5.56 mM glucose, 4.17 mM $NaHCO_3$, pH 7.2, all from Sigma-Aldrich), and then were loaded with 1 μM Fluo-4 AM (Life Technologies Hungary Ltd.) dissolved in Hank's solution (100 μl/well) at 37°C for 30 min. The cells were then washed three times with Hank's solution (100 μl/well). The plates were then placed into a FlexStation 3 multi-mode microplate reader (Molecular Devices) and alterations of the cytoplasmic Ca^{2+} concentration (reflected by changes in fluorescence; λ_{EX}: 490 nm, λ_{EM}: 520 nm) were monitored at room temperature following the application of OEA or vehicle. In order to probe reactivity and viability of the cells, at the end of each measurement, 0.2 mg/ml ATP was administered as a positive control. Data are presented as F/F_0, where F_0 is the average baseline fluorescence (i.e. before compound application), whereas F is the actual fluorescence.

siRNA Transfection-Mediated Selective Gene Silencing Of GPR119

Human SZ95 sebocytes were seeded in (d=35 mm) Petri dishes or in 96-well "black well/clear bottom" plates (Greiner Bio-One) in culture medium. On the other day, medium was changed, and the cells were transfected with siRNA oligonucleotides targeting human GPR119 (Stealth RNA_i, assay IDs: HSS134803, HSS134804, and HSS134805; Life Technologies Hungary Ltd.) using Lipofectamine® RNA_i MAX Transfection Reagent and serum-free Opti-MEM™ (both form ThermoFisher). For controls, siRNA Negative Control Duplexes with "medium" GC ratio (SCR, ThermoFisher) were employed. Silencing efficiency was monitored on post-transfection Days 2 and 3 at the mRNA (Q-PCR) and protein (Western blot) levels, respectively. In our preliminary experiments, we found that among the above three siRNA constructs, only one (HSS134805) was able to efficiently silence the expression of GPR119. In our hands, HSS134803 was not efficient, whereas the effect of HSS134804 could only be detected on post-transfection Day 2, but not on Day 3 (data not shown). Thus, in our subsequent experiments we used only HSS134805.

Statistical Analysis

Data were analyzed by *IBM SPSS Statics software version 20* (IBM Armonk, North Castle, NY, USA), or *GraphPad Prism 8.3.1 (549)* (GraphPad Software , LLC, San Diego, CA, USA) using Student's two-tailed, unpaired *t*-test (paired comparisons) or one-way ANOVA with Bonferroni's *post hoc* test (multiple comparisons) and $P<0.05$ values were regarded as significant differences. Graphs were plotted using *Origin Pro Plus 6* software (Microcal, Northampton, MA, USA) or *GraphPad Prism 8.3.1 (549)*.

SUPPLEMENTARY DISCUSSION

As mentioned in the main text, the recently de-orphanized, "ECS-related" GPR119 receptor has lately emerged as a promising therapeutic target in T2DM. Although the tested synthetic agonists have not passed yet phase II clinical trials (Yang et al. 2018), the promising animal data continuously encourage development and testing of novel GPR119 activators (Tyurenkov et al. 2017). Of great importance, however, both endogenous and synthetic agonists of GPR119 may exhibit biologically relevant signaling bias (Hassing et al. 2016), preferring one potential second messenger system over the others, and due to such bias, biological effects of the individual activators may be different. Thus, our data do not necessarily mean that all GPR119 agonists would promote sebaceous lipogenesis of human sebocytes. However, in case of those ones, which exhibit the highest similarities in their second messenger pathway profiles with the endogenous ligand OEA, risk of such adverse effects cannot be excluded (supposing that they reach sufficiently high concentration in the sebaceous glands).

SUPPLEMENTARY FIGURES

Supplementary Figure S1 *Up to 50 μM, OEA does not decrease viability of human SZ95 sebocytes*

MTT-assays. Viability of SZ95 sebocytes was monitored following 24- (**a**), and 48-hr (**b**) treatments. Results are expressed in the percentage of the vehicle control (100%, solid line) as mean±SEM of four independent determinations. Two additional experiments yielded similar results. **OEA:** oleoylethanolamide.

Supplementary Figure S2 *Up to 50 μM, OEA does not influence proliferation of human SZ95 sebocytes*

CyQUANT proliferation assay. SZ95 sebocytes were plated at low (2,000/well) initial cell count to enable rapid proliferation. Cell count was assessed following 48-hr treatments. Results are expressed in the percentage of the 24-hr vehicle control (100%, solid line) as mean±SEM of four independent determinations. Two additional experiments yielded similar results. **OEA:** oleoylethanolamide.

Supplementary Figure S3 *Positive control staining for GPR119*

(**a**-**b**) Immunohistochemistry of human pancreas was performed as described in the **Supplementary Materials & Methods**. Specific immunopositivity was visualized by 3,3'-diaminobenzidine (DAB; brown color), whereas nuclei were counterstained by hematoxylin (blue color). Original magnification: 400x; scale bars: 50 μm. Negative control (**b**) was obtained by omitting the primary antibody.

Supplementary Figure S4 *Higher non-cytotoxic concentrations of OEA further promote sebaceous lipogenesis; however, at 500 µM, OEA reduces viability of human sebocytes*

(**a**) Nile Red assay. Lipogenesis of SZ95 sebocytes was assessed following 24-hr treatments. Results are expressed in the percentage of the vehicle control (100%, solid line) as mean±SEM of twelve independent determinations. ** and *** mark significant (P<0.01 and 0.001, respectively) difference compared to the control group. n.s.: not significant, as indicated. (**b**) MTT-assay. Viability of SZ95 sebocytes was monitored following 24-hr treatments. Results are expressed in the percentage of the vehicle control (100%, solid line) as mean±SEM of twelve independent determinations. ** and *** mark significant (P<0.01 and 0.001, respectively) difference compared to the control group. n.s.: not significant, as indicated. **OEA:** oleoylethanolamide.

Supplementary Figure S5 *OEA does not influence Ca^{2+}-homeostasis of human SZ95 sebocytes*

Fluo-4 AM-based fluorescent Ca^{2+}-measurement. Compounds (first OEA or vehicle, and then ATP as positive control) were applied as indicated by the respective arrows. Fluorescence (measured in relative fluorescence units) was normalized to the baseline. The graph shows a representative data set performed in octuplicate. **OEA:** oleoylethanolamide.

Supplementary Figure S6 *Full, uncropped western blot membranes demonstrating GPR119 expression*

(**a**) Expression of GPR119 in pre- and post-confluent sebocyte cultures (**Figure 3c**). (**b-c**) Selective gene silencing of GPR119 (**Figure 3f**). Expression of GPR119 (**b**) and the loading control β-actin (**c**). Red rectangles indicate the relevant parts, which have been presented on **Figure 3c** and **3f**.

Supplementary Figure S7 *Full, uncropped western blot membranes demonstrating ERK1/2 phosphorylation*

(**a**) Phospho-ERK1/2. (**b**) β-tubulin (loading control). (**c**) ERK1/2. (**d**) β-tubulin (loading control). Red rectangles indicate the relevant parts, which have been presented on **Figure 4a**.

SUPPLEMENTARY TABLES

Supplementary Table S1 *Relevant anamnestic data of the acne and acne-free patients, whose skin samples were used to assess GPR119 expression*

Acne-free patients (pigmented nevus)			**Acne patients**		
Age	Sex	Region	Age	Sex	Region
25	male	back	22	male	back
20	male	back	37	male	back
19	male	back	17	male	back
22	male	back	no data	male	back
17	male	back	no data	male	back
28	male	back	no data	male	back

SUPPLEMENTARY REFERENCES

Green DR, Reed JC. Mitochondria and apoptosis. Science. 1998;281(5381):1309–12

Sakamoto Y, Inoue H, Kawakami S, Miyawaki K, Miyamoto T, Mizuta K, et al. Expression and distribution of Gpr119 in the pancreatic islets of mice and rats: predominant localization in pancreatic polypeptide-secreting PP-cells. Biochem. Biophys. Res. Commun. 2006;351(2):474–80

Schindelin J, Arganda-Carreras I, Frise E, Kaynig V, Longair M, Pietzsch T, et al. Fiji: an open-source platform for biological-image analysis. Nat. Methods. 2012;9(7):676–82

Susin SA, Zamzami N, Kroemer G. Mitochondria as regulators of apoptosis: doubt no more. Biochim Biophys Acta. 1998;1366(1-2):151-165

Yang JW, Kim HS, Choi Y-W, Kim Y-M, Kang KW. Therapeutic application of GPR119 ligands in metabolic disorders. Diabetes Obes Metab. 2018;20(2):257–69